Optics Letters

Experimental demonstration of a single silicon ring resonator with an ultra-wide FSR and tuning range

Ang Li[1,2,*] and Wim Bogaerts[1,2]

[1]Photonics Research Group, Ghent University-IMEC, Department of Information Technology, Ghent University, Ghent 9052, Belgium
[2]Center for Nano- and Biophotonics, Ghent University, Ghent 9052, Belgium
*Corresponding author: ang.li@Ugent.be

Received 20 September 2017; revised 2 November 2017; accepted 2 November 2017; posted 3 November 2017 (Doc. ID 307167); published 29 November 2017

We present an experimental realization of a pseudo single-mode silicon ring resonator with an ultra-wide free spectral range and tuning range. The device is a single microring resonator with a tunable reflector integrated inside. The reflector is designed to have zero reflection for only one resonance of the ring, while all other resonances will suffer strong reflection. Given that the reflection inside a ring resonator leads to resonance splitting and degradation of the extinction ratio (ER), we obtain a ring resonator where only a single resonance has a large ER, while all others have a very low ER. The large ER resonance can be continuously tuned using metal heaters to achieve a broad tuning range over 55 nm with 16 mW of power injected into the phase shifter.

OCIS codes: (140.3490) Lasers, distributed-feedback; (060.2420) Fibers, polarization-maintaining; (060.3735) Fiber Bragg gratings.

https://doi.org/10.1364/OL.42.004986

Silicon microring resonators can be found in many applications of integrated optics. Silicon rings can have an ultra-compact size, exhibit a large *extinction ratio* (ER), a wide *free spectral range* (FSR), and a high quality (Q) factor, etc. [1–7]. Even with the compact size of silicon rings, the operation range is often limited to a single FSR. There is still a need for ring resonators with a wider FSR (>30 nm), as this allows more wavelength channels for ring-based (de-)multiplexers [8], a broader working range for ring-based integrated sensors [6], and a wider operation span for single-mode laser cavities that also frequently employ ring resonators [9]. Currently, the FSR can be increased by three different means. Reducing the ring's radius is the most straightforward method as the FSR is reversely proportional to the ring's total roundtrip length. However, the length cannot be infinitely reduced as a tight bend radius shorter than 5 μm in silicon photonics will be problematic in many ways. It will not only make the light more sensitive to the sidewall roughness, but also cause extra reflections at the bend-straight interfaces [10–12]. Moreover, these extremely sharp bends make it difficult to engineer the coupling section for a specific coupling strength without resorting to impractically narrow gaps [13,14] that are hard to fabricate and will cause extra coupling loss and coupler-induced backscattering to the circuit [2,12]. So far, the smallest silicon ring resonator fabricated with acceptable performance has a radius of 1.5 μm with an FSR around 45 nm [14].

Two alternative, more complicated methods, have been proposed to increase the FSR. One can take advantage of the Vernier effect present in multiple ring resonators with slightly different FSRs [15]. However, the use of multiple rings will raise the fabrication variation and complexity, as resonances of each ring need to be precisely tuned. It also complicates the control, as the two rings need to be independently controlled. Another approach is to add intentional reflections inside the ring cavity to suppress or cancel the side modes with only one mode left [16,17]. Two techniques have been reported based on this approach. Urbonas *et al.* deposited metal nanodisks along the ring waveguide [16]. Even while an ultra-wide FSR can be generated, the existence of metal adds significant loss to the ring cavity. As a consequence, the ER and Q factor of the resonance are limited to less than 3 dB and 300, respectively. Huang *et al.* demonstrated a sidewall Bragg grating along the ring waveguide to achieve a pseudo single-mode condition [17]. Such a Bragg grating is not simple to design so that it is spectrally correctly aligned with the required resonances of the ring. It can be tuned with roughly the same tuning efficiency as a single silicon ring resonator around 370 nm/refractive index unit (RIU). If an integrated heater is used to shift the resonance, a 100 K change in the temperature can only lead to a resonance shift around 7 nm, as the thermo-optic coefficient of silicon is around 1.8×10^{-4} [18].

In Ref. [19], we theoretically proposed a novel ring resonator shown in Fig. 1 with an integrated reflector, where both the ring and the reflector can be independently tuned over a wide range. In this Letter, we present the experimental implementation and validation of this device concept, fully integrated on a silicon photonics platform and effectively demonstrating an ultra-wide FSR and tuning range using simple thermo-optic heaters. The measured FSR is more than 100 nm, and this

number is only limited by the tunable laser source used for characterization. In addition, a 55 nm tuning range is achieved with only 16 mW of power consumed by the metal heaters. This value can be further improved by more efficient heaters.

In our previous paper, Ref. [19], we give a very comprehensive elaboration of the working principle of the ring resonator, and its performance is simulated for various sets of design parameters. In general, our approach can be considered as one of the techniques based on internal reflections in a ring resonator to suppress all resonances but one. Instead of using metal nanodisks or a sidewall Bragg grating, we implement an integrated tunable reflector as a loop-ended Mach–Zehnder interferometer (MZI), as shown in Fig. 1. The reflector provides diverse reflection spectra, depending on its configuration [20]; an example is shown in Fig. 2, where a broad optical span (>100 nm) shows only a single wavelength point at 1530 nm with zero reflection. Over the rest of the wavelength span, there is strong reflection. The zero-reflection wavelength point is designed following equation Eq. (1):

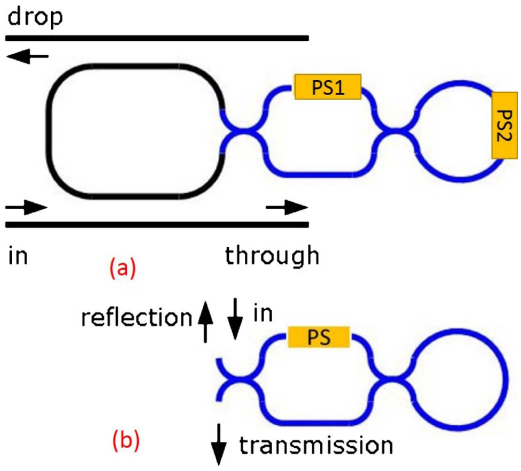

Fig. 1. Schematic of (a) our device and (b) the tunable reflector. The device is a single-ring resonator with a tunable reflector inside. The reflector is a sub-circuit based on a loop-ended MZI with tunable *phase shifters* (PS). The MZI is designed to be unbalanced with a length difference ΔL.

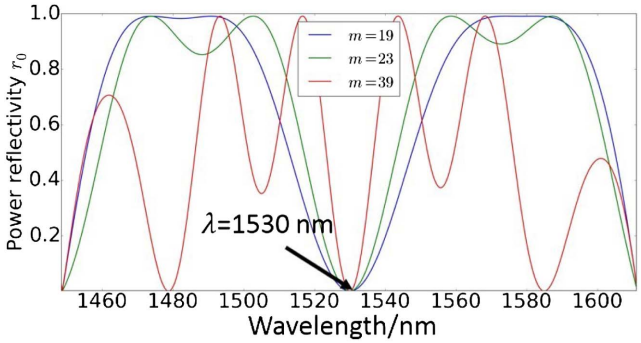

Fig. 2. Simulated reflection spectrum of the tunable reflector. Over a very wide wavelength range, only a single wavelength point has 0 reflection. Larger order m leads to a sharper slope, but it cannot be too large in order to avoid extra dips.

$$\frac{2\pi\Delta L n_{\text{eff}}}{\lambda} = m\pi. \tag{1}$$

ΔL refers to the length difference between the two arms of the MZI. n_{eff} is the effective index of the waveguide at λ, λ is the zero-reflection wavelength point, and m is the interference order of the MZI. As shown in Fig. 2, a larger m will lead to a sharper slope around the 0 wavelength point, which is beneficial for a larger side mode suppression ratio (SMSR), but it will decrease the FSR and, therefore, limit the wavelength range for single-resonance operation. In our model, both waveguide dispersion and directional coupler dispersion are included.

The unique reflection spectrum of the wavelength-dependent loop mirror allows us to create an ultra-wide FSR ring resonator when we use the reflection spectrum to suppress the ER of all resonances, except one Fig. 3 [19]. For this, we need to align the zero-reflection wavelength with one of the ring resonances and, as a consequence, only this resonance will have a large ER while all the rest will show a very limited ER, making this ring resonator pseudo single mode with an ultra-wide FSR. The simulated spectrum for $m = 19$ is shown in Fig. 4.

In terms of the tunability, we can achieve a wide tuning range by two-step tuning. First, the zero-reflection wavelength of the reflector can be tuned by adding a phase shift onto one arm of the MZI (PS1 in Fig. 1). The wavelength shift versus index change of the arm is given in Eq. (2):

$$\frac{\Delta\lambda}{\lambda_0} = \frac{\Delta n}{n_g}\frac{L_{\text{ps1}}}{\Delta L}. \tag{2}$$

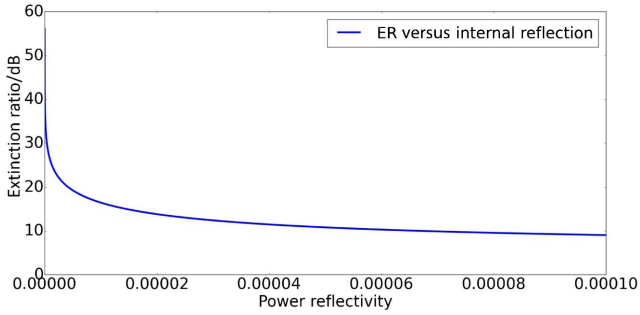

Fig. 3. This plot shows the ER of a ring resonance as a function of the power reflectivity of a lumped reflector inside the ring cavity. The ER can be dramatically suppressed with increasing power reflectivity.

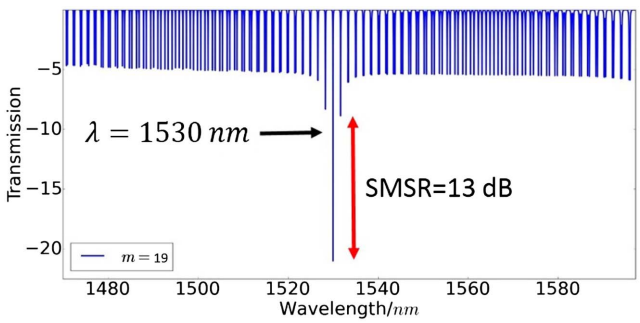

Fig. 4. Simulated spectrum of the complete device with different interference orders of the MZI reflector. Within an ultra-wide range, only one resonance is left.

$\Delta\lambda$ is the shift of the zero-reflection wavelength λ_0 caused by index change Δn in PS1 with a length of L_{ps1}, and n_g is the group index of the waveguide. The shift distance at a given index change is much larger than that of a normal silicon ring resonance [given in Eq. (3)] due to the amplification coefficient $\frac{L_{ps1}}{\Delta L}$. For instance, if L_{ps1} is designed to be 100 μm and $\Delta L = 7.3$ μm (corresponding with $m = 23$), the tuning range of the zero-reflection wavelength is 14× larger than a normal silicon ring resonance with the same index change Δn:

$$\frac{\Delta\lambda}{\lambda_0} = \frac{\Delta n}{n_g}. \tag{3}$$

The second step is then to slightly shift the complete ring spectrum using PS2 in Fig. 1 to make one resonance well aligned with the zero-reflection wavelength. The simulated spectra are given in Fig. 5. A 100 K change in the temperature ($\Delta n = 0.018$) can make the resonance shift over 80 nm, which is 12× larger than a normal silicon ring resonator.

The devices shown in Fig. 6 are fabricated in IMEC's 200 mm pilot line through the Europractice MPW service [21]. The substrate is a 220 nm thick silicon-on-insulator wafer, and the devices are covered by a 1.5 μm thick planarized silicon dioxide layer, on top of which the integrated metal heaters are processed in the Ghent University clean rooms. Each heater consists of a titanium resistive element with 2 μm width and 100 nm thickness. The metal wires are based on gold with 10 μm width and 500 nm thickness. All the waveguides are designed to have a width at 450 nm to ensure single-mode operation. Grating couplers are employed to achieve fiber-chip coupling. The bend radius in the ring and routing waveguide are defined to be 5 μm to avoid unwanted reflections and radiation loss. The m factor of the reflector is designed to be 19. For the measurement, we use an Agilent tunable laser (1465–1570 nm) to perform the wavelength sweep, and the two metal heaters (PS1 and PS2) are driven by two Keithley 2400 source meters independently. PS1 is responsible for shifting the zero-reflection wavelength of the reflector, while PS2 is in charge of shifting the ring spectrum. In Fig. 7, we give the measured spectra of our device when PS1 = 0 mW, meaning no power is injected into phase shifter 1. By tuning PS2 to the correct condition, where one of the ring resonances matches the zero-reflection point (around 1505 nm), the SMSR improves. The designed zero-reflection point is 1480 nm. This deviation is due to the fabrication variation that influences the effective

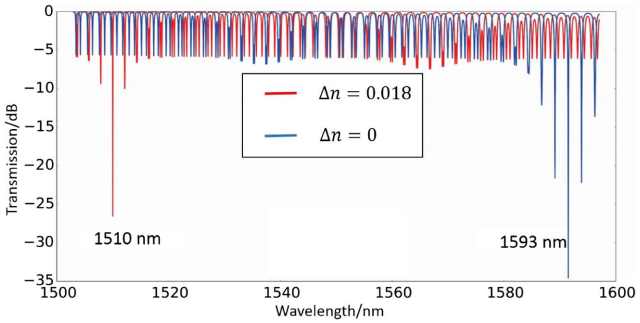

Fig. 5. Refractive index change of 0.018 (corresponding to a 100 K change in temperature in silicon) will generate a resonance shift over 80 nm. This is 12× larger than a normal silicon ring resonator.

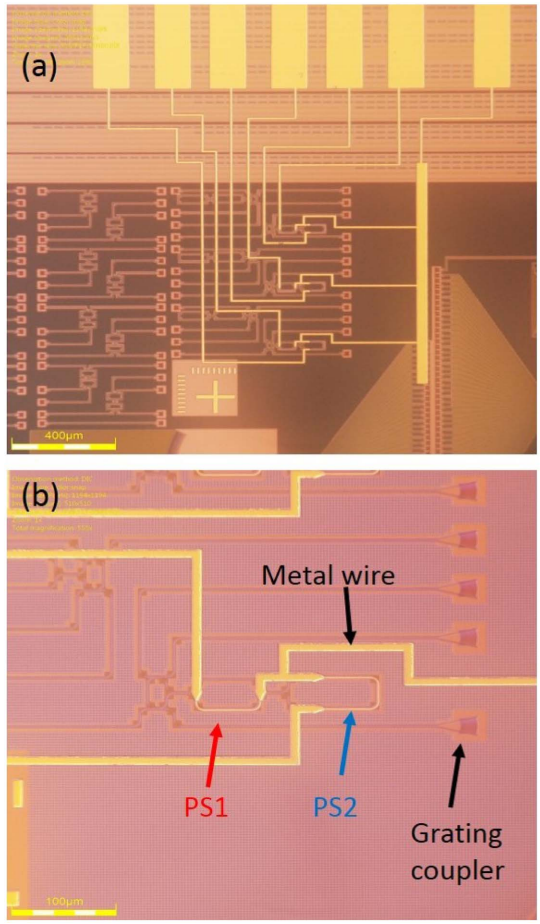

Fig. 6. Microscope images of the fabricated device with (a) integrated phase shifters (metal heaters) and (b) a zoom view of a single device.

index of the waveguides. The optimized SMSR here is about 12 dB, but it can be further improved by multiple methods.

- The current ring roundtrip length is excessively long, as each arm of the reflector is 200 μm to ensure an adequate phase shift. A long roundtrip leads to a small FSR, which means the side mode is closer to the single mode, so a smaller SMSR is present. However, each arm can be reduced to less than 100 μm with enough phase shift (at least 2π). The total length will be optimized to only 60% of the current value, meaning the FSR will be increased by one-and-a-half times. This will significantly increase the spacing of the side modes, thus increasing the SMSR.
- As demonstrated in our previous theoretical paper [19], SMSR can be further increased by increasing the coupling coefficient of the ring resonator at the price of a lower Q factor.
- Also discussed in the theoretical paper [19], SMSR can be further increased by increasing the m factor of the reflector; in this way, the slope of the reflection spectrum will be sharpened. However, increasing m will slightly decrease the tuning range and, if it is too large, an extra zero reflection point will be generated in the reflection spectrum. Thus, there is some compromise.

In Fig. 8, we show the shift of the single mode by injecting power into PS1. Still, PS2 needs to be controlled to get a good alignment between the ring resonance and the zero-reflection

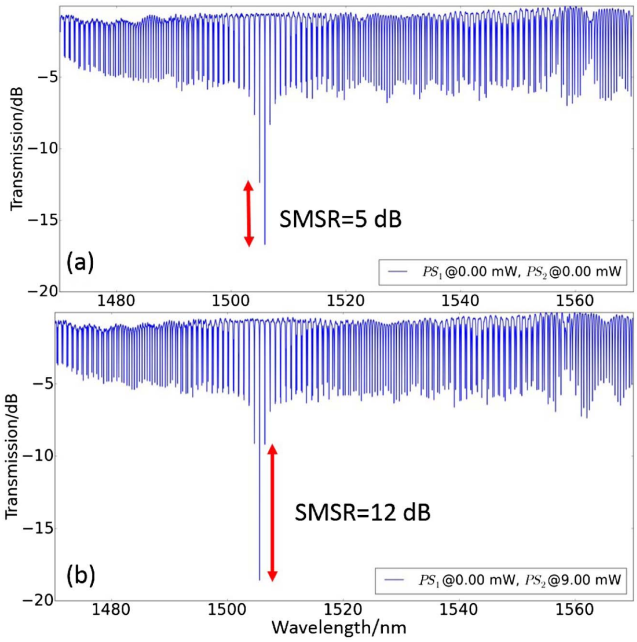

Fig. 7. Measured spectra of our device. (a) Shows the condition that the ring resonance does not match the zero-reflection point perfectly and (b) gives the results when PS2 is tuned so that one resonance is well aligned to the zero-reflection point.

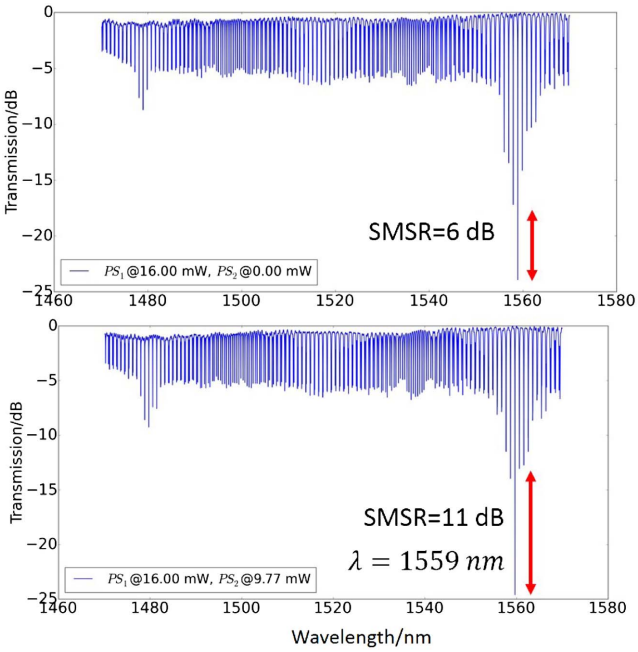

Fig. 8. By controlling PS1, the zero-reflection point can be shifted. Then tuning PS2 will again make one resonance match it to get a good ER and SMSR. 16 mW (around 0.0148 index change) can shift the single mode around 55 nm, which is 11× more efficient than a normal silicon ring resonator.

point. The measured results show that 16 mW can shift the resonance around 55 nm. According to Ref. [22], 18 mW for a titanium heater leads to a temperature change around 93 K (corresponding index change 0.0167). Thus, 16 mW can roughly generate an index change of 0.0148. Compared to a normal silicon ring resonator, such an index change will only shift the ring resonance around 5.5 nm, assuming the group index to be 4.2. Usually, the maximum power injected into a metal heater is limited, so this indicates that our device has a 11× wider tuning range than a normal silicon ring resonator if the same heaters are employed.

In summary, we present the experimental demonstration of our previous design of a silicon ring resonator with an ultra-wide FSR and tuning range. The principle is to take advantage of a unique integrated tunable reflector to suppress all the ring resonances but one. In the measured 100 nm span (limited by our laser source), only one resonance has a large ER, while the rest gets suppressed by this internal reflector. The SMSR is measured to be over 12 dB, which is enough for applications such as optical sensors and microwave photonics. [6,23] Moreover, given the same index change or power consumed by a phase shifter, it can provide an 11× wider tuning range, compared to a normal silicon ring resonator.

REFERENCES

1. S. J. Emelett and R. Soref, J. Lightwave Technol. **23**, 1800 (2005).
2. F. Xia, L. Sekaric, and Y. A. Vlasov, Opt. Express **14**, 3872 (2006).
3. W. Bogaerts, P. De Heyn, T. Van Vaerenbergh, K. De Vos, S. Kumar Selvaraja, T. Claes, P. Dumon, P. Bienstman, D. Van Thourhout, and R. Baets, Laser Photon. Rev. **6**, 47 (2012).
4. Q. Xu and M. Lipson, Opt. Express **15**, 924 (2007).
5. A. Malacarne, F. Gambini, S. Faralli, J. Klamkin, and L. Poti, IEEE Photon. Technol. Lett. **26**, 1042 (2014).
6. J.-W. Hoste, S. Werquin, T. Claes, and P. Bienstman, Opt. Express **22**, 2807 (2014).
7. A. Li and W. Bogaerts, APL Photon. **2**, 096101 (2017).
8. B. E. Little, J. Foresi, G. Steinmeyer, E. Thoen, S. Chu, H. Haus, E. Ippen, L. Kimerling, and W. Greene, IEEE Photon. Technol. Lett. **10**, 549 (1998).
9. B. Liu, A. Shakouri, and J. E. Bowers, IEEE Photon. Technol. Lett. **14**, 600 (2002).
10. S. K. Selvaraja, W. Bogaerts, and D. Van Thourhout, Opt. Commun. **284**, 2141 (2011).
11. H. Shen, L. Fan, J. Wang, J. C. Wirth, and M. Qi, IEEE Photon. Technol. Lett. **22**, 1174 (2010).
12. A. Li, T. Vaerenbergh, P. Heyn, P. Bienstman, and W. Bogaerts, Laser Photon. Rev. **10**, 420 (2016).
13. M. S. Nawrocka, T. Liu, X. Wang, and R. R. Panepucci, Appl. Phys. Lett. **89**, 71110 (2006).
14. A. M. Prabhu, A. Tsay, Z. Han, and V. Van, IEEE Photon. Technol. Lett. **21**, 651 (2009).
15. T. Claes, W. Bogaerts, and P. Bienstman, Opt. Express **18**, 22747 (2010).
16. D. Urbonas, A. Balčytis, M. Gabalis, K. Vaškevičius, G. Naujokaitė, S. Juodkazis, and R. Petruškevičius, Opt. Lett. **40**, 2977 (2015).
17. Q. Huang, K. Ma, and S. He, IEEE Photon. Technol. Lett. **27**, 1402 (2015).
18. J. Komma, C. Schwarz, G. Hofmann, D. Heinert, and R. Nawrodt, Appl. Phys. Lett. **101**, 041905 (2012).
19. A. Li, Q. Huang, and W. Bogaerts, Photon. Res. **4**, 84 (2016).
20. A. Li and W. Bogaerts, Opt. Express **25**, 2092 (2017).
21. P. P. Absil, P. Verheyen, P. De Heyn, M. Pantouvaki, G. Lepage, J. De Coster, and J. Van Campenhout, Opt. Express **23**, 9369 (2015).
22. P. Dong, R. Shafiiha, S. Liao, H. Liang, N.-N. Feng, D. Feng, G. Li, X. Zheng, A. V. Krishnamoorthy, and M. Asghari, Opt. Express **18**, 10941 (2010).
23. J. Dong, L. Liu, D. Gao, Y. Yu, A. Zheng, T. Yang, and X. Zhang, IEEE Photon. J. **5**, 5500307 (2013).